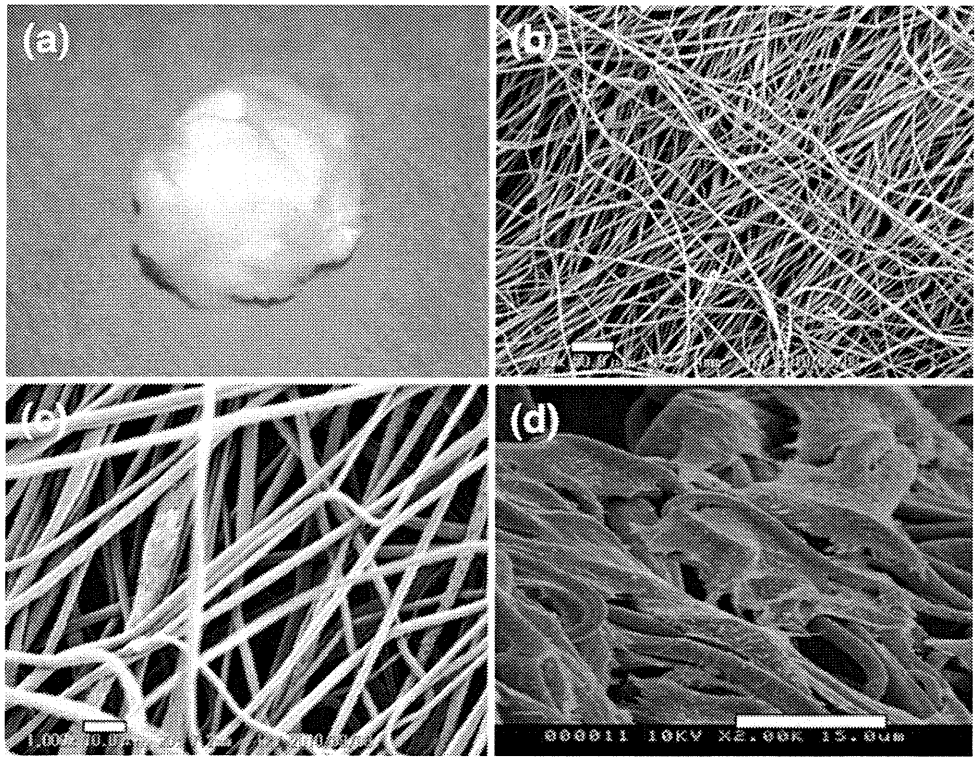

FIGURE 1. (a) Overall appearance of SRBFS. SRBFS appears to have a "cotton wool"-like formation. (b) SEM (original magnification, ×200) of SRBFS reveals a non-woven fabric appearance. Scale bar: 50 μm. (c) SEM (original magnification, ×1000) of SRBFS showed that the polymer fiber was 500 μm-10 nm in diameter. Scale bar: 10 μm. (d) FESEM image of BMSCs seeded on SRBFS after 7 days. Scale bar: 15 μm.

10% FBS and 1% penicillin/streptomycin for 7 or 14 days in a humidified environment with 5% CO_2 at 37 °C before *in vitro* assays and cultured for 14 days before *in vivo* assays, with the medium changed every 3 days. Osteogenic factors, such as dexamethasone and BMP-2, were not added in the culture medium during the culture period.

Scanning Electron Microscopic Study

BMSCs cultured on SRBFS for 7 days were washed with PBS to remove non-adherent cells, fixed in 2.5% glutaraldehyde, and then post-fixed in 4% osmium tetroxide. The samples were dehydrated through a series of graded alcohol solutions. After *t*-butyl-alcohol freeze-drying, cellular constructs were sputter-coated with osmium and observed under field emission scanning electron microscopy (FESEM) (S-800, Hitachi, Tokyo, Japan) at 10 kV.

Measurement of Alkaline Phosphatase Activity

Seven and 14 days after seeding on BFS and SRBFS, BMSCs were assayed for alkaline phosphatase (ALP) activity. ALP activity was measured with a commercial *p*-nitrophenyl phosphate tablet set (Sigma Chemical, St. Louis, MO, USA) and a cell counting kit (WST-8: Dojindo, Kumamoto, Japan). Cell numbers were analyzed according to the manufacturer's protocol. Briefly, 100 μL of reagents was added to each well containing 1 mL of fresh medium with cell-scaffold constructs, incubated for 3 h, and absorbance measured on a spectrophotofluorometer (Bio-Rad Laboratories, Hercules, CA, USA). Cell numbers were determined from the standard calibration curve by measuring the absorbance. After WST-8 analysis, each well and scaffolds were washed three times with PBS, and 800 mL of *p*-nitrophenyl phosphate solution was added to each well. After 10 min of incubation at 37 °C, the reaction was stopped with 800 mL of 3 N NaOH and the absorbance of *p*-nitrophenol was measured. ALP activities were normalized to the number of cells calculated according to the WST-8 assay.

In Vitro Osteoclast Formation

Mouse osteoclasts were prepared from bone marrow cells as previously described.[25] Briefly, bone marrow cells were obtained by flushing the femurs and tibiae of mice and cultured in α-MEM containing 10% FBS for 1 day. Non-adherent cells were harvested and cultured in α-MEM (5×10^4 cells per well in a 24-well

plate) with 10% FBS containing 10 ng/mL M-CSF (R&D Systems, Inc., Minneapolis, MN, USA). Two days later, adherent cells were used as bone marrow-derived monocyte/macrophage precursor cells (BMMs) after washing out the non-adherent cells. These cells were cultured with 100 ng/mL RANKL (R&D Systems, Inc., Minneapolis, MN, USA) and 10 ng/mL M-CSF (R&D Systems), and co-cultured with 5 mg of SRBFS or BFS. Indirect co-culture systems for BMMs and SRBFS or BFS were established using a 24-well plate with 0.4-μm pore, 10-μm thickness polyester membrane cell culture inserts (Corning, NY, USA). BMMs were cultured on the plate well, and SRBFS or BFS were then placed in the insert. After 5 days, cultured cells were fixed and stained for tartrate-resistance acid phosphatase (TRAP) (Wako Pure Chemical Industries, Osaka, Japan). TRAP-positive multinucleated cells with greater than three nuclei were counted as osteoclasts.

Cell-Scaffold Construct Implantation

After the mice were anesthetized by diethyl ether inhalation (Sigma-Aldrich, Tokyo, Japan), small incisions were made on the bilateral dorsal skin. A cell-seeded SRBFS was immediately implanted into the left subcutaneous pocket on the murine back, a cell-seeded BFS into the right, and the skin was then closed with sutures.

Radiographic Analysis

Twelve weeks after transplantation, the samples were assessed by X-ray (G1 meisterII FLUOREX, Toshiba, Tokyo, Japan), and the conditions used were 40 kV and 200 mA for 0.640 s. Under these defined conditions, exposures were carried out with an aluminum wedge that allowed the radiographic densities to be computed later. The radiographic density of the harvested transplant area was estimated as aluminum thickness by measuring with image analysis software (Image J, Scion Corporation, Frederick, MD, USA).

Histological Analysis of Ectopic Bone Formation In Vivo

Six and 12 weeks after transplantation, the implants were harvested for analysis, immediately fixed in 4% (w/v) paraformaldehyde and decalcified with a commercially available decalcifying solution (K-CX, Falma Corporation, Tokyo, Japan) for about 2 days before embedding in paraffin. Three-micrometer serial sections were cut and processed for routine histological observation by staining with hematoxylin and eosin (H–E) and for immunochemistry. The bone formation area was measured using image analysis software (Image J, Scion Corporation, Frederick, MD, USA), and then expressed as the percentage of bone area in the total cross-sectional area. Immunohistochemical analysis was performed using bone sialoprotein (BSP) polyclonal antibody (1:200) (LSL Co., Cosmo Bio, Tokyo, Japan) as primary antibody. A biotinylated secondary antibody (1:200) (rabbit anti-mouse IgG) (Vector Laboratories, CA, USA) was applied, and an avidin–biotin complex using Vectastain ABC kit (Vector Laboratories). Finally, slides were reacted with 0.1% w/v 3,3′-diaminobenzidine tetrahydrochloride solution and counterstained with hematoxylin solution. The BSP-positive cells were counted as follows. At least 10 fields for each section were randomly captured (×200 magnification, 5 samples in total), and then all cells and BSP depositing cells in the fields were counted. The ratio of BSP-positive cells was calculated as the percentage of BSP-positive cells in all cells.

Mineralization Analysis

Bone mineralization was analyzed by determining the amount of deposited calcium using a method reported previously.[14] Twelve weeks after transplantation, retrieved implant samples were rinsed with PBS and homogenized with 0.6 N HCl, and calcium was then extracted by shaking them for 4 h at 4 °C. The lysate was then centrifuged at 1,000×g for 5 min, and the supernatant was used to quantify calcium content in samples by spectrophotometry using a Calcium Colorimetric Assay Kit (BioVision, Mountain View, CA, USA). Five minutes after the addition of reagents, the absorbance of the samples was read at 575 nm using a microplate reader (SmartSpeckTM3000, Bio-Rad, Tokyo, Japan). Calcium content was calculated from a standard curve generated from the serial dilution of a calcium standard solution (BioVision).

Statistical Analysis

Statistical significance was analyzed either by one-way factorial analysis of variance (ANOVA) or unpaired t test. A p value less than 0.05 was considered statistically significant. Quantitative data were statistically analyzed to express the mean ± the standard deviation.

RESULTS

Morphology of BMSCs on SRBFS

The FESEM image of BMSCs cultured on SRBFS for 7 days shows that the cells spread actively, rigidly

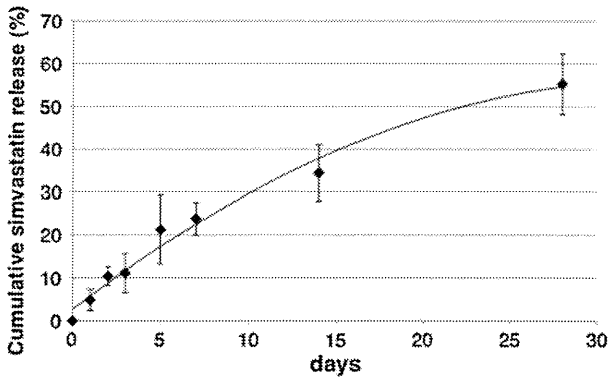

FIGURE 2. Cumulative release of SRBFS *in vitro*. The curve is intended to lead the eye. Values represent the mean ± standard deviation ($n = 3$).

adhered to the fibers, and ECM production by cells was then observed (Fig. 1d).

In Vitro Simvastatin Release from SRBFS

The *in vitro* release pattern of simvastatin from SRBFS is shown in Fig. 2. On day 1, approximately 5% of the simvastatin was released from SRBFS. Thereafter, simvastatin release was slow and at a constant rate until day 7. By day 14, about 35% of the loaded simvastatin was released, and about 55% of it from SRBFS by day 28.

Effect of Released Simvastatin on BMSC Osteogenic Differentiation

To examine whether released simvastatin had an effect on osteogenic differentiation of BMSCs, ALP activity was measured *in vitro* on days 7 and 14 (Fig. 3). Although there was no significant difference between the SRBFS and BFS groups on day 7, the ALP activity of the SRBFS groups was significantly higher than that of the BFS groups ($p < 0.05$) on day 14.

Effect of Released Simvastatin on Inhibition of Osteoclastogenesis

The effect of simvastatin released from SRBFS on osteoclastogenesis was examined. Figures 4a and 4b revealed that BMMs incubated with BFS differentiated into many osteoclasts, whereas BMMs incubated with SRBFS differentiated into only a few osteoclasts. As shown in Fig. 4c, the total number of TRAP-positive multinucleated osteoclasts in the SRBFS group was significantly inhibited compared with the BFS group.

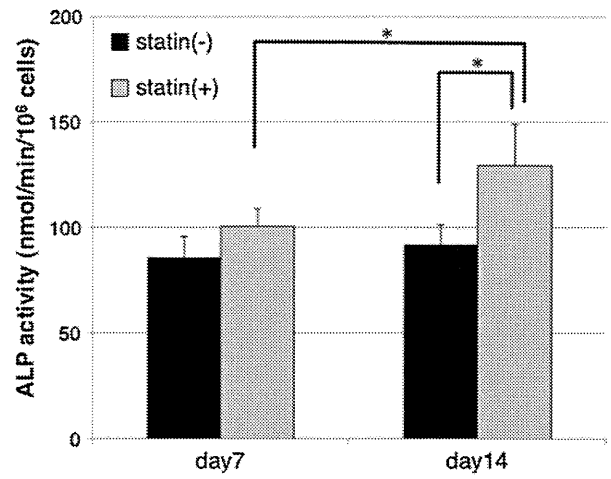

FIGURE 3. ALP activity of BMSCs on SRBFS and BFS measured on days 7 and 14. Values represent the mean ± standard deviation ($n = 5$). Statistically significant difference is labeled ($^*p < 0.05$).

Radiographic Analysis

Figure 5a shows X-ray photographs 12 weeks after transplantation. Round-shaped radiopaque tissues were found on both sides. Statistical analysis showed that SRBFS radiodensity was significantly higher than in the BFS group 12 weeks after transplantation (Fig. 5b).

Histological and Immunohistochemical Analysis

Figures 6a–6d show H–E staining sections 6 and 12 weeks after transplantation. Six weeks after transplantation, an extensive immature mineral formation had been observed in both groups (Figs. 6a, 6b). At 12 weeks, mainly woven bone and focal trabecular bone with a lamellar appearance were observed. Numerous osteoblasts lining the woven bone and mineral formation indicated active bone formation (Figs. 6c, 6d). Immunohistochemical staining with BSP was performed using the section harvested from implants taken from mice (Figs. 6e, 6f). BSP was positive in a wide range of intracellular and extracellular tissue regardless of statin content. Newly formed bone area and the ratio of BSP-positive cells in the SRBFS groups were significantly higher than those in the BFS groups 12 weeks after implantation (Figs. 7a, 7b).

Mineralization Analysis

To determine the mineralized matrix deposition in the generated tissue, calcium deposition was measured. Calcium deposition in the SRBFS group was higher than in the BFS group (Fig. 7c).

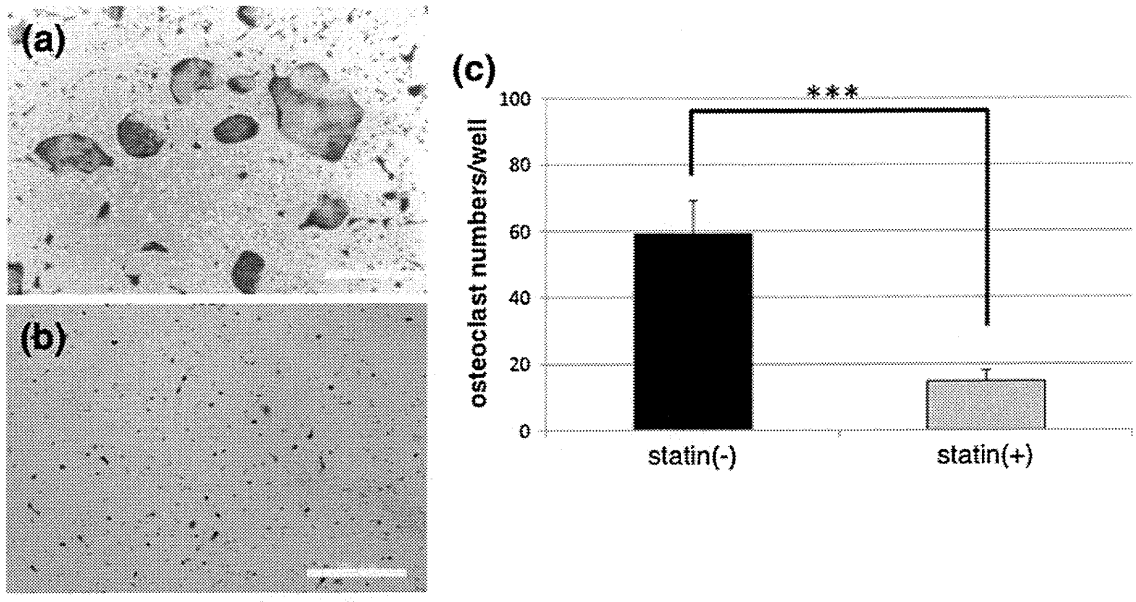

FIGURE 4. Simvastatin released from SRBFS inhibits RANKL-induced osteoclastogenesis 5 days after stimulation. Cells were cultured for 5 days with (a) SRBFS and (b) BFS after RANKL treatment and stained for TRAP expression. Scale bar: 500 μm. (c) The total number of TRAP-positive multinucleated osteoclasts (i.e., those containing three nuclei) per well were counted. Values represent the mean ± standard deviation ($n = 5$). Statistically significant difference is labeled (*$p < 0.001$).**

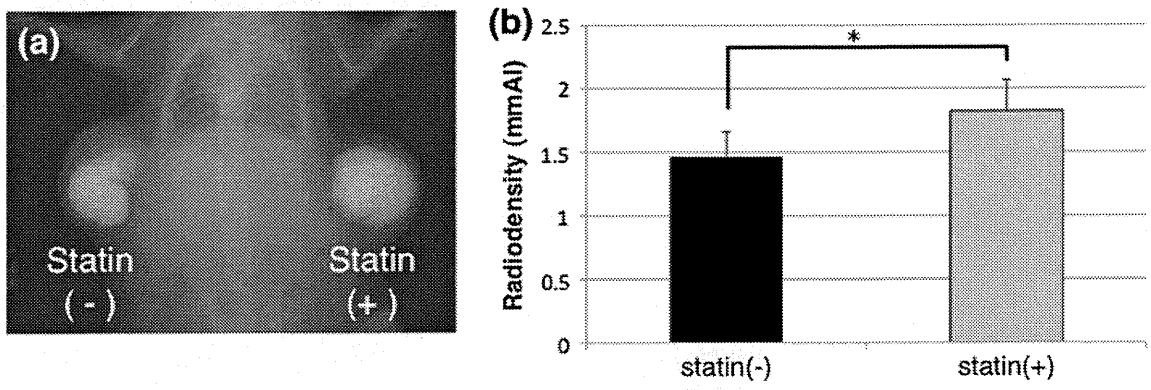

FIGURE 5. (a) X-ray photograph of ectopically formed bone 12 weeks after transplantation. (b) Radiographic density in the transplants 12 weeks after transplantation ($n = 4$). Values represent the mean ± standard deviation. Statistically significant difference is labeled (*$p < 0.05$).

DISCUSSION

Our current study is the first report to describe the ectopic bone formation of mice using the complex of statin-releasing biodegradable nano- to microscaled fiber scaffolds and BMSCs, and our scaffold is applicable for bone tissue engineering.

Our *in vitro* studies revealed that the effects of simvastatin released from SRBFS on osteoblastogenesis and osteoclastogenesis were effective for osteogenesis. ALP activity of BMSCs seeded on the SRBFS for 2 weeks was significantly elevated, and the number of osteoclasts differentiated from precursor cells was significantly decreased in the SRBFS. Thus, we demonstrated that simvastatin released from SRBFS promotes simultaneously osteoblastic differentiation of BMSCs and inhibits osteoclastogenesis of BMMs. However, in this study, the inhibition of osteoclastogenesis was demonstrated only *in vitro*, and further *in vivo* assays are needed to evaluate in more detail the effect of simvastatin on osteoclastogenesis.

In several previous studies, the simvastatin was loaded in various materials for bone tissue engineering, such as gelatin hydrogel,[26] α-tricalcium phosphate,[17] methylcellulose gel,[23] collagen sponge,[28] and calcium sulfate.[18] Most of these studies reported positive effects for bone regeneration. In this study, the statin-loaded biodegradable fiber from the electrospinning procedure was developed to release the simvastatin gradually over

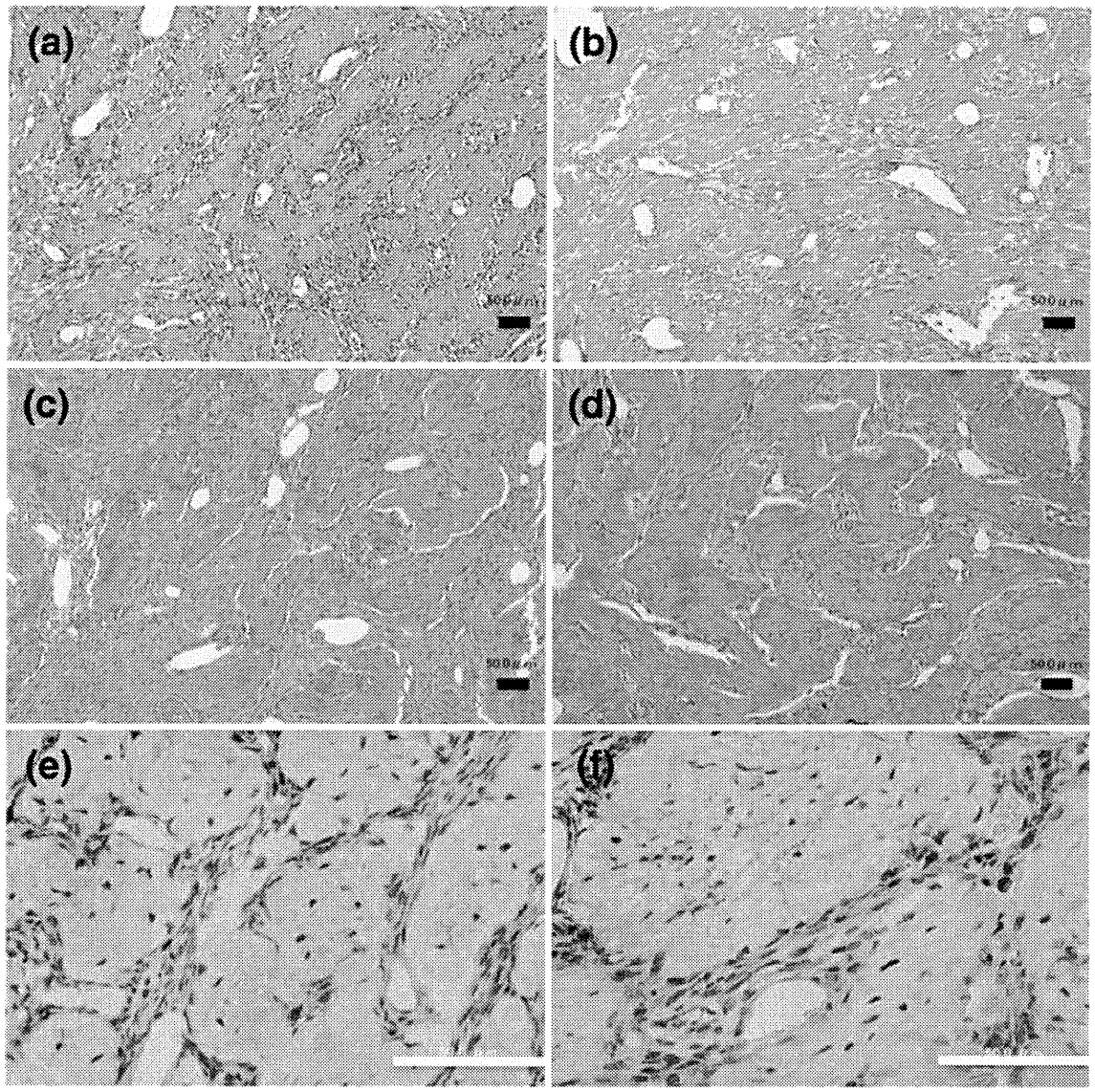

FIGURE 6. Histological and immunohistochemical analyses 6 and 12 weeks after implantation. (a–d) H–E staining, (a, b) at 6 and (c, d) 12 weeks, while (e, f) show immunohistochemical staining with BSP at 12 weeks. (a, c, e): BFS (b, d, f): SRBFS. Scale bar: 50 μm.

time. The mechanism of sustained release of simvastatin takes place through degradation of biodegradable polymer by hydrolysis. The electrospinning procedure makes it possible to control the release of a wide range of antibiotics[5] and anticancer drugs[30] to proteins[9,16] and DNA[16] for application in tissue engineering. However, this technique has a limitation in that some organic solvents used to prepare the polymer solutions may also degrade the drugs.[1]

To optimize this simvastatin-releasing system, we determined the simvastatin content of SRBFS on the basis of the simvastatin release test of SRBFS and preliminary studies. BMSCs were cultured in various concentrations (0.5–5.0 μM) of simvastatin, and cell proliferation and ALP activity were then evaluated. These preliminary studies suggested that the appropriate concentration of simvastatin was 0.5–1 μM in *in vitro* culture with respect to cell proliferation (cytotoxicity) and ALP activity (data not shown). BMSCs could not proliferate in a medium containing more than 2.5 μM of simvastatin. Though the apoptotic effect of high-dose simvastatin has been reported in several studies,[6,7] more than a certain concentration of simvastatin is apparently needed for osteogenic induction and osteoclastogenesis inhibition. However, it is difficult to measure exactly a local simvastatin-exposed dose to cells with such direct adhesion to fiber as in this study. Besides the simvastatin content of the biodegradable polymer, the dose of simvastatin released from fibers is also dependent on the composition

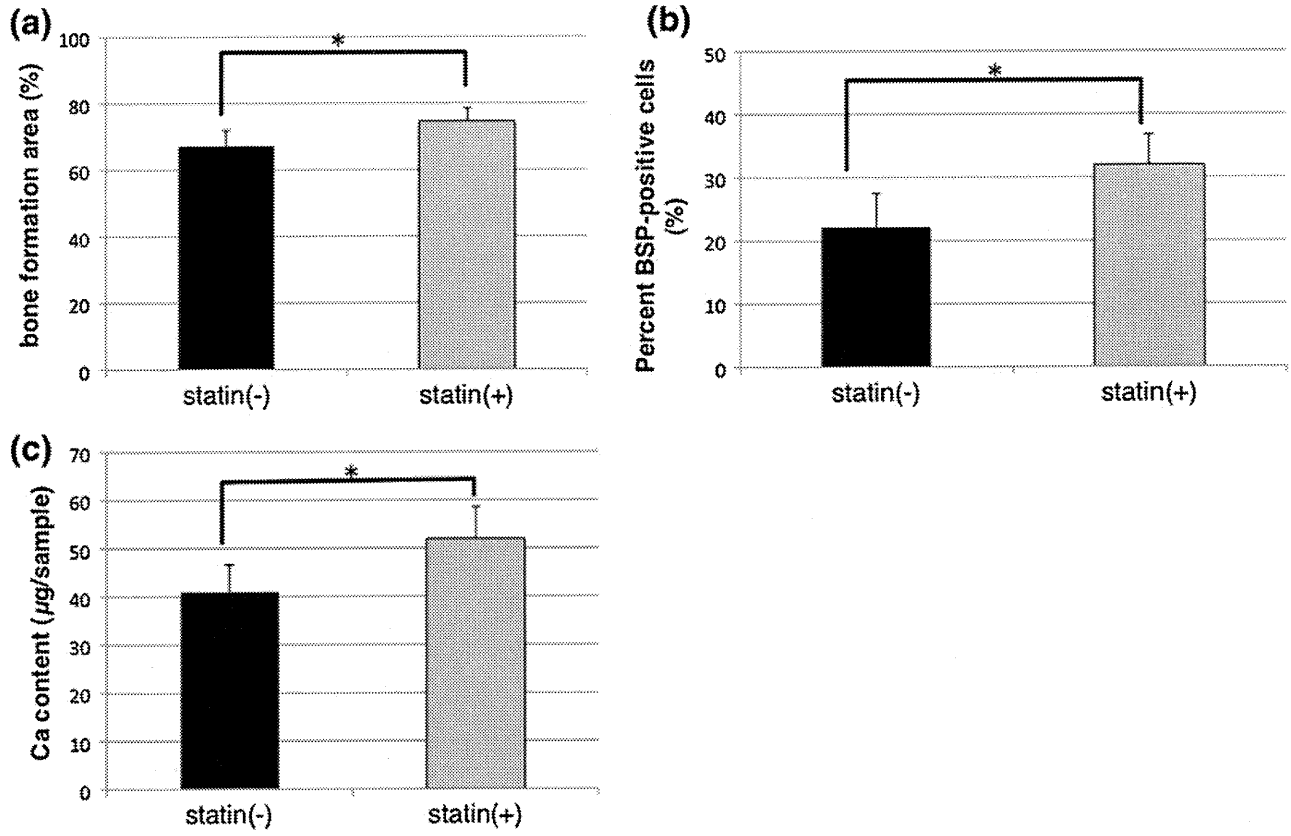

FIGURE 7. (a) Bone formation area analyzed by H&E staining 12 weeks after implantation ($n = 5$). (b) Percent BSP-positive cells as determined by immunohistochemical staining with BSP 12 weeks after implantation ($n = 5$). (c) Accumulated calcium content per sample 12 weeks after implantation ($n = 4$). Values represent the mean ± standard deviation. Statistically significant difference is labeled ($^*p < 0.05$).

of the polymer (polyglycolic acid (PGA), polylactic acid (PLA), polycaplolacton (PCL), and their co-polymers), along with the rate of copolymerization, and fiber diameter. These factors need to be taken into consideration for optimization of drug release in the future. If the local dose of statin released from the scaffold can be regulated appropriately, this strategy could not only minimize damage to cells at high concentrations, but also reduce the drug dosage needed, and thereby be more effective, safe and inexpensive for bone tissue engineering.

Histological examination 12 weeks after transplantation revealed that the amount of new bone formation in the SRBFS group was significantly higher than in the BFS group. Twelve weeks after transplantation, SRBFS alone without BMSCs did not induce bone formation in the murine back (data not shown). These data suggest that BMSCs could play an important role in ectopic bone formation, and statin may promote the osteogenic activity of BMSCs for bone formation. To the best of our knowledge, successful ectopic bone formation *in vivo* using statin-releasing materials without cell transplantation has not been reported in detail. A previous study reported that statin-loaded biodegradable fiber without seeding cells was applied for healing a critical-size bone defect of an animal,[19] and suggested the necessity of cell-seeded scaffolds. While statin alone was insufficient to induce ectopic bone formation, in combination with preosteogenic cells statin resulted in significant promotion of such formation.

Analyses of radiodensity and calcium deposition were performed to determine the mineralized matrix deposition in scaffolds. Some studies reported that local application of statin could increase bone mineral density.[17,29] Our results reveal that the SRBFS group showed significantly higher mineralization, which suggests that statin may play a pivotal role in mineralization during bone maturation. The osteogenic phenotype of BMSCs seeded onto SRBFS was also assessed by the immunodetection of a specific osteoblastic protein, BSP. High BSP expression confirms the presence of mature osteoblasts.[4] These results suggest that released simvastatin may also promote bone maturation as well as osteogenic induction.

Our results demonstrate that the combination of BMSCs and biodegradable fiber scaffolds releasing simvastatin, which acts like an osteoinductive factor,

may be an excellent strategy for bone tissue engineering applications. We here combined simvastatin-releasing materials with cell transplantation to a bone tissue engineering scaffold in an attempt to form new ectopic bone. This "cotton wool"-like configuration fiber scaffold can flexibly fit any shape of a local bone defect site. Furthermore, the present result of ectopic bone formation *in vivo* shows that this strategy has potential for application to large bone defects under severe conditions. Although its clinical utility for large bone defects is limited by its relatively poor mechanical properties, these can be improved by combination with other materials.

In summary, our data suggest that sustained simvastatin release from biodegradable nano-microfiber scaffolds promotes osteogenic differentiation of BMSCs and enhances new bone formation *in vivo*.

ACKNOWLEDGMENTS

This work was supported by a grant-in-aid for "Young Scientists (start up)" (20890100) from the Ministry of Education, Culture, Sports, Science, and Technology of Japan, and by a grant for "COE for Education and Research of Micro-Nano Mechatronics Nagoya University Global COE Program."

REFERENCES

[1]Ahmad, Z., H. B. Zhang, U. Farook, M. Edirisinghe, E. Stride, and P. Colombo. Generation of multilayered structures for biomedical applications using a novel tri-needle coaxial device and electrohydrodynamic flow. *J. R. Soc. Interface* 5:1255–1261, 2008.

[2]Ahn, K. S., G. Sethi, M. M. Chaturvedi, and B. B. Aggarwal. Simvastatin, 3-hydroxy-3-methylglutaryl coenzyme A reductase inhibitor, suppresses osteoclastogenesis induced by receptor activator of nuclear factor-kappaB ligand through modulation of NF-kappaB pathway. *Int. J. Cancer* 123:1733–1740, 2008.

[3]Badami, A. S., M. R. Kreke, M. S. Thompson, J. S. Riffle, and A. S. Goldstein. Effect of fiber diameter on spreading, proliferation, and differentiation of osteoblastic cells on electrospun poly(lactic acid) substrates. *Biomaterials* 27:596–606, 2006.

[4]Bianco, P., M. Riminucci, E. Bonucci, J. D. Termine, and P. G. Robey. Bone sialoprotein (BSP) secretion and osteoblast differentiation: relationship to bromodeoxyuridine incorporation, alkaline phosphatase, and matrix deposition. *J. Histochem. Cytochem.* 41:183–191, 1993.

[5]Bolgen, N., I. Vargel, P. Korkusuz, Y. Z. Menceloglu, and E. Piskin. In vivo performance of antibiotic embedded electrospun PCL membranes for prevention of abdominal adhesions. *J. Biomed. Mater. Res. B Appl. Biomater.* 81:530–543, 2007.

[6]Fromigue, O., E. Hay, D. Modrowski, S. Bouvet, A. Jacquel, P. Auberger, and P. J. Marie. RhoA GTPase inactivation by statins induces osteosarcoma cell apoptosis by inhibiting p42/p44-MAPKs-Bcl-2 signaling independently of BMP-2 and cell differentiation. *Cell Death Differ.* 13:1845–1856, 2006.

[7]Garcia-Roman, N., A. M. Alvarez, M. J. Toro, A. Montes, and M. J. Lorenzo. Lovastatin induces apoptosis of spontaneously immortalized rat brain neuroblasts: involvement of nonsterol isoprenoid biosynthesis inhibition. *Mol. Cell. Neurosci.* 17:329–341, 2001.

[8]Hwang, C. J., A. R. Vaccaro, J. P. Lawrence, J. Hong, H. Schellekens, M. H. Alaoui-Ismaili, and D. Falb. Immunogenicity of bone morphogenetic proteins. *J. Neurosurg. Spine* 10:443–451, 2009.

[9]Jiang, H., Y. Hu, P. Zhao, Y. Li, and K. Zhu. Modulation of protein release from biodegradable core-shell structured fibers prepared by coaxial electrospinning. *J. Biomed. Mater. Res. B Appl. Biomater.* 79:50–57, 2006.

[10]Krebsbach, P. H., S. A. Kuznetsov, K. Satomura, R. V. Emmons, D. W. Rowe, and P. G. Robey. Bone formation in vivo: comparison of osteogenesis by transplanted mouse and human marrow stromal fibroblasts. *Transplantation* 63:1059–1069, 1997.

[11]Mundy, G., R. Garrett, S. Harris, J. Chan, D. Chen, G. Rossini, B. Boyce, M. Zhao, and G. Gutierrez. Stimulation of bone formation in vitro and in rodents by statins. *Science* 286:1946–1949, 1999.

[12]Mutsuga, M., Y. Narita, A. Yamawaki, M. Satake, H. Kaneko, Y. Suematsu, A. Usui, and Y. Ueda. A new strategy for prevention of anastomotic stricture using tacrolimus-eluting biodegradable nanofiber. *J. Thorac. Cardiovasc. Surg.* 137:703–709, 2009.

[13]Mutsuga, M., Y. Narita, A. Yamawaki, M. Satake, H. Kaneko, A. Usui, and Y. Ueda. Development of novel drug-eluting biodegradable nano-fiber for prevention of postoperative pulmonary venous obstruction. *Interact. Cardiovasc. Thorac. Surg.* 8:402–406, 2009 (discussion 406–407).

[14]Nagano, M., T. Kitsugi, T. Nakamura, T. Kokubo, and M. Tanahashi. Bone bonding ability of an apatite-coated polymer produced using a biomimetic method: a mechanical and histological study in vivo. *J. Biomed. Mater. Res.* 31:487–494, 1996.

[15]Nakase, T., and H. Yoshikawa. Potential roles of bone morphogenetic proteins (BMPs) in skeletal repair and regeneration. *J. Bone Miner. Metab.* 24:425–433, 2006.

[16]Nie, H., and C. H. Wang. Fabrication and characterization of PLGA/HAp composite scaffolds for delivery of BMP-2 plasmid DNA. *J. Control Release* 120:111–121, 2007.

[17]Nyan, M., D. Sato, H. Kihara, T. Machida, K. Ohya, and S. Kasugai. Effects of the combination with alpha-tricalcium phosphate and simvastatin on bone regeneration. *Clin. Oral Implants Res.* 20:280–287, 2009.

[18]Nyan, M., D. Sato, M. Oda, T. Machida, H. Kobayashi, T. Nakamura, and S. Kasugai. Bone formation with the combination of simvastatin and calcium sulfate in critical-sized rat calvarial defect. *J. Pharmacol. Sci.* 104:384–386, 2007.

[19]Piskin, E., I. A. Isoglu, N. Bolgen, I. Vargel, S. Griffiths, T. Cavusoglu, P. Korkusuz, E. Guzel, and S. Cartmell. In vivo performance of simvastatin-loaded electrospun spiral-wound polycaprolactone scaffolds in reconstruction of cranial bone defects in the rat model. *J. Biomed. Mater. Res. A* 90:1137–1151, 2009.

[20]Shimer, A. L., F. C. Oner, and A. R. Vaccaro. Spinal reconstruction and bone morphogenetic proteins: open questions. *Injury* 40(Suppl 3):S32–S38, 2009.
[21]Sill, T. J., and H. A. von Recum. Electrospinning: applications in drug delivery and tissue engineering. *Biomaterials* 29:1989–2006, 2008.
[22]Song, C., Z. Guo, Q. Ma, Z. Chen, Z. Liu, H. Jia, and G. Dang. Simvastatin induces osteoblastic differentiation and inhibits adipocytic differentiation in mouse bone marrow stromal cells. *Biochem. Biophys. Res. Commun.* 308:458–462, 2003.
[23]Stein, D., Y. Lee, M. J. Schmid, B. Killpack, M. A. Genrich, N. Narayana, D. B. Marx, D. M. Cullen, and R. A. Reinhardt. Local simvastatin effects on mandibular bone growth and inflammation. *J. Periodontol.* 76:1861–1870, 2005.
[24]Stevens, M. M. Biomaterials for bone tissue engineering. *Mater. Today* 11:18–25, 2008.
[25]Takayanagi, H., S. Kim, T. Koga, H. Nishina, M. Isshiki, H. Yoshida, A. Saiura, M. Isobe, T. Yokochi, J. Inoue, E. F. Wagner, T. W. Mak, T. Kodama, and T. Taniguchi. Induction and activation of the transcription factor NFATc1 (NFAT2) integrate RANKL signaling in terminal differentiation of osteoclasts. *Dev. Cell* 3:889–901, 2002.
[26]Tanigo, T., R. Takaoka, and Y. Tabata. Sustained release of water-insoluble simvastatin from biodegradable hydrogel augments bone regeneration. *J. Control Release* 143:201–206, 2010.
[27]Venugopal, J., Y. Z. Zhang, and S. Ramakrishna. Fabrication of modified and functionalized polycaprolactone nanofibre scaffolds for vascular tissue engineering. *Nanotechnology* 16:2138–2142, 2005.
[28]Wong, R. W., and A. B. Rabie. Histologic and ultrastructural study on statin graft in rabbit skulls. *J. Oral Maxillofac. Surg.* 63:1515–1521, 2005.
[29]Wu, Z., C. Liu, G. Zang, and H. Sun. The effect of simvastatin on remodelling of the alveolar bone following tooth extraction. *Int. J. Oral Maxillofac. Surg.* 37:170–176, 2008.
[30]Xie, J., and C. H. Wang. Electrospun micro- and nanofibers for sustained delivery of paclitaxel to treat C6 glioma in vitro. *Pharm. Res.* 23:1817–1826, 2006.
[31]Yamawaki-Ogata, A., R. Hashizume, M. Satake, H. Kaneko, S. Mizutani, T. Moritan, Y. Ueda, and Y. Narita. A doxycycline loaded, controlled-release, biodegradable fiber for the treatment of aortic aneurysms. *Biomaterials* 31:9554–9564, 2010.
[32]Zhang, Y., H. Ouyang, C. T. Lim, S. Ramakrishna, and Z. M. Huang. Electrospinning of gelatin fibers and gelatin/PCL composite fibrous scaffolds. *J. Biomed. Mater. Res. B Appl. Biomater.* 72:156–165, 2005.

進行口腔癌に対する逆行性超選択的動注化学放射線療法

光藤健司[1)] 岩井俊憲[1)] 光永幸代[1)]
小栗千里[1)] 小泉敏之[1)] 來生知[1)]
廣田誠[1)] 玉利正之[2)] 山本憲幸[2)]
上田実[2)] 藤内祝[1)]

要 旨

進行口腔癌に対する逆行性超選択的動注化学療法は放射線療法との連日同時併用が可能となることから高い抗腫瘍効果が得られる。今回われわれは進行口腔癌に対して根治的逆行性超選択的動注化学放射線療法を施行し，治療効果，累積生存率，局所制御率について検討したので報告する。

2003年1月から2009年12月に受診した口腔・顎顔面悪性腫瘍688例中，根治的逆行性超選択的動注化学放射線療法を施行した175症例を対象とした。治療は逆行性超選択的動注化学放射線療法（docetaxel, total 60mg/m^2, cisplatin, total 125-150mg/m^2, total 50-60Gy）を5～6週間行った。治療4週後に画像検索および原発の生検にて腫瘍残存の有無の確認を行ったところ，175例中160例（91.4%）がCR，腫瘍残存は15例（8.6%）に認めた。CRであった160例についてはその後の経過観察中に14例（8.0%）の再発を認めた。5年累積生存率および局所制御率はそれぞれ71.6%と82.2%であった。

キーワード：進行口腔癌，逆行性超選択的動注法，化学放射線療法，累積生存率，局所制御率

Chemoradiotherapy using retrograde superselective intra-arterial infusion for advanced oral cancer:

Kenji Mitsudo[1)], Toshinori Iwai[1)], Sachiyo Mitsunaga[1)], Senri Oguri[1)], Toshiyuki Koizumi[1)], Mitomu Kioi[1)], Makoto Hirota[1)], Masayuki Tamari[2)], Noriyuki Yamamoto[2)], Minoru Ueda[2)] and Iwai Tohnai[1)]

[1)] Department of Oral and Maxillofacial Surgery, Yokohama City University Graduate School of Medicine

[2)] Department of Oral and Maxillofacial Surgery, Nagoya University Graduate School of Medicine

Summary

Concurrent chemoradiotherapy using retrograde superselective intra-arterial infusion demonstrates good local control and overall survival rates due to the advantage of simultaneous infusion of anticancer agent with the synergistic effects of chemotherapy and radiotherapy. This study evaluated the therapeutic results, overall survival and local control rates in patients with advanced oral cancer treated with definitive concurrent chemoradiotherapy using retrograde superselective intra-arterial infusion.

A total of 688 patients with carcinoma of the head and neck were referred to our institution between January 2001 and December 2006. Among them, 175 patients with carcinoma of the oral cavity underwent definitive concurrent chemoradiotherapy using retrograde superselective intra-arterial infusion. Treatment consisted of superselective intra-arterial infusions (docetaxel, total 60 mg/m^2, cisplatin, total 125-150 mg/m^2) and daily concurrent radiotherapy (total 50-60 Gy) for 5-6 weeks. Four weeks after the completion of all treatments, patients underwent biopsy of the primary lesion and radiological examinations. Complete response (CR) of the primary site was achieved in 160 (91.4%) of the 175 patients. Residual disease at the primary site was seen in 15 patients (8.6%), and 14 patients (8.0%) showed local recurrence during follow-up. Five-year survival and local control rates were 71.6% and 82.2%, respectively.

Key words : Advanced oral cancer, Retrograde superselective intra-arterial infusion, Chemoradiotherapy, Overall survival rate, Local control rate

[Received Aug. 3, 2011, Accepted Sept. 1, 2011]

[1)] 横浜市立大学大学院医学研究科顎顔面口腔機能制御学
[2)] 名古屋大学大学院医学系研究科顎顔面外科学
[平成23年8月3日受付，平成23年9月1日受理]

別刷請求先：〒236-0004 神奈川県横浜市金沢区福浦3-9
横浜市立大学大学院医学研究科顎顔面口腔機能制御学
光藤 健司

はじめに

頭頸部癌に対する超選択的動注法は大腿動脈経由のSeldinger法（以下Seldinger法）[1-3]と浅側頭動脈，後頭動脈よりの逆行性超選択的動注法[4-6]に分類される。逆行性超選択的動注法は放射線療法との連日同時併用が可能となることから高い抗腫瘍効果が得られ，これまでにわれわれは進行口腔癌に対し術前治療として逆行性超選択的動注化学療法，連日同時放射線併用療法（以下，動注CCRT）を施行し，良好な治療成績につき報告した[7]。さらに現在では臓器，機能温存を目的とした原発部位の手術回避も可能となっている[8]。今回われわれは根治的動注CCRTを施行した進行口腔癌における治療効果，累積生存率，局所制御率，有害事象について検討したので報告する。

対象と方法

2003年1月から2009年12月の6年間に横浜市立大学附属病院歯科口腔外科，名古屋大学医学部附属病院歯科口腔外科を受診した口腔・顎顔面悪性腫瘍688例中，根治的動注CCRTを施行し治療が完遂できた175症例を対象とした。年齢は28歳から91歳，性別は男性106例(60.6%)，女性69例（39.4%），原発部位は舌67例（38.2%），上顎歯肉34例（19.4%），下顎歯肉30例（17.1%），頬粘膜18例（10.3%），口底15例（8.6%），硬口蓋4例（2.3%），口唇2例（1.1%），その他5例であった（表1）。治療開始時には175例すべてに遠隔転移は認めなかった。Stage分類はstage Ⅱ：40例（22.9%），stage Ⅲ：41例（23.4%）stage Ⅳ：94例（53.7%）とstage Ⅳが半数以上であった（表2）。

治療前に3 dimensional CT angiography（3D-CTA）を用いて腫瘍の栄養動脈および栄養動脈の解剖学的検索を行った。浅側頭動脈よりの超選択的動注カテーテル留置術はFuwaら[4,9]，Tohnaiら[5,10]の方法に従って行い，2007年以降は複数の栄養動脈を有する進行口腔癌に対しては浅側頭動脈および後頭動脈よりの同時カテーテル留置術を行った[6]。カテーテル留置後はangio-CT，digital subtraction angiography（DSA）の撮影を行い，腫瘍への血流を確認した。また週に1回，インジゴカルミンを用いて腫瘍への血流を確認した。抗癌剤はdocetaxcel（DOC）を10mg/m^2/week，cisplatin（CDDP）を5 mg/m^2/dayとし，動注カテーテルを2本留置している場合には抗癌剤を半量ずつとした。治療スケジュールはDOCとCDDPの2剤を投与する場合は各抗癌剤を1時間ずつ計2時間にて投与し，その間に放射線治療を行い，CDDP1剤を投与する場合はCDDPを1時間で投与し，同様にその間に放射線治療を行った。根治的動注CCRT（DOC：60mg/m^2，CDDP：125-150mg/m^2，50-60Gy）を5～6週間施行し，治療終了4週間後に画像検索および原発部位の生検を行い，治療効果判定を行った。頸部リンパ節転移を認める症例に対しては原則として頸部郭清術を行った（図1）。

治療中および治療終了4週間後までの有害事象(粘膜炎，皮膚炎，好中球減少，血小板減少，貧血，クレアチニン，発熱）をNational Cancer Institute-Common Terminology Criteria for Adverse Events v3.0.（CTCAE v3.0）日本語訳JCOG/JSCO版に従って検討した。

表1　根治的動注CCRTを施行した口腔癌175症例の原発部位

原発部位	症例数	%
舌	67	38.2
上顎歯肉	30	19.4
下顎歯肉	30	17.1
頬粘膜	18	10.3
口底	15	8.6
硬口蓋	4	2.3
口唇	2	1.1
その他	5	2.9

表2　根治的動注CCRTを施行した口腔癌175症例のStage分類

Stage	症例数	%
Stage Ⅱ	40	22.9
Stage Ⅲ	41	23.4
Stage Ⅳ	94	53.7

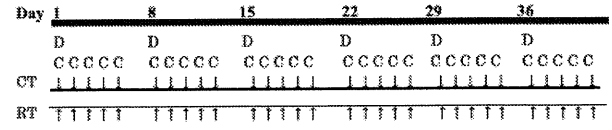

CT：Chemotherapy using intra-arterial infusion
D: Docetaxel 10mg/m²/week: bolus infusion (Total 60mg/m²)
C: Cisplatin 5 mg/m²/day: bolus infusion (Total 125-150mg/m²)
RT：Radiotherapy 2 Gy/day (Total: 60Gy)
（頸部リンパ節転移症例 ⟶ 頸部郭清術）

図1　根治的動注CCRTの治療スケジュール

結　果

根治的動注CCRTを施行した175症例中160例(91.4%)がCR，15例（8.6%）に腫瘍残存を認めた。CRであった160例についてはその後の経過観察中，14例（8.0%）に原発の再発を認めた。175症例中133例は生存，45例は死亡した。死亡原因は遠隔転移26例，原発，頸部の非制御11例，他病死8例であった。3年，5年累積生存率はそれぞれ75.9%，71.6%，3年，5年局所制御率はともに82.2%であった（図2）。

治療中および治療終了4週間後までの有害事象を表3に示す。Grade 3，4の重篤な有害事象は粘膜炎148例(84.6%)，皮膚炎35例（20.0%），好中球減少症33例(18.9%)，血小板減少症7例(4.0%)，貧血29例(16.6%)，

発熱13例（7.4%），嘔吐21例（12.0%）であった。有害事象による死亡例はなかった。

考　察

頭頸部癌に対し臓器温存のために化学放射線療法を選択することが多くなっており，プラチナ製剤，フッ化ピリミジン系の代謝拮抗剤，タキサン系抗癌剤などの多剤を用いた同時化学放射線療法（Concurrent chemoradiotherapy）のトライアルも報告された[11-13]。当科ではstage Ⅰ，Ⅱ口腔癌に対しては通常原発巣の切除術を原則としているが，late T2症例，手術拒否症例に対しては動注CCRTを適応することもある。局所進行口腔癌であっても根治的動注CCRTを施行することによって高い局所制御率を示し，機能温存が可能となった[8]。表4に頭頸部癌，口腔癌に対する超選択的動注化学放射線療法の生存率，局所制御率，局所・所属リンパ節制御率を示す。Robbinsら[14]はstage Ⅳの頭頸部癌61症例，Hommaら[3]は頭頸部癌43症例，Kobayashiら[15]は口腔癌22症例に対し，Seldinger法による動注化学放射線療法を行ったところ，3年生存率はそれぞれ56.2%，54.0%，78.5%であった。また，3年局所・所属リンパ節制御率は57.2%[14]，68.9%[3]であった。われわれがstage Ⅱ，Ⅲ，Ⅳの口腔癌に対して根治的動注CCRTを施行した175症例の3年累積生存率，局所制御率はそれぞれ75.9%，82.2%と良好な結果であった。

われわれが根治的動注CCRTを施行したところ，grade 3，4の粘膜炎は84.6%に認めたが，皮膚炎，血液毒性，腎機能障害，嘔吐については20%以下であった。表5にこれまでに報告されている頭頸部癌，口腔癌症例に対する根治的動注化学放射線療法を行った際の有害事象を示す。Robbinsら[14]はstage Ⅳの頭頸部癌症例に対してRADPLATを用いて治療を行ったところgrade 3，4の粘膜炎を58%に認め，grade 3，4の血液毒性を49%，grade 5を2%に認めた。Hommaら[3]はstage Ⅲ，Ⅳの頭頸部癌に対して同様にRADPLATを用いて治療を行ったところgrade 3，4の粘膜炎を37.2%に認め，grade 3，4の好中球減少症，血小板減少症，貧血はそれぞれ27.9%，2.3%，4.7%であった。Kobayashiら[15]は22症例の進行口腔癌に対し，nedaplatinとDOCによるSeldinger法による動注

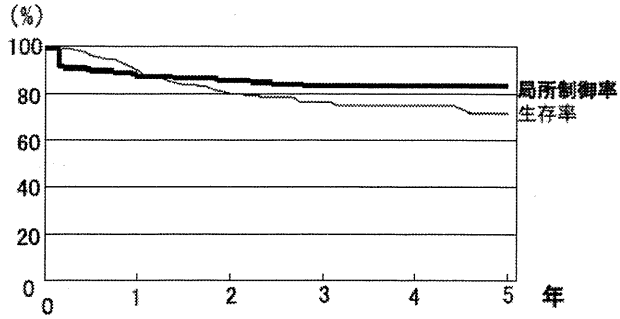

図2　根治的動注CCRTを施行した口腔癌175症例の累積生存率（細線）と局所制御率（太線）

表3　根治的動注CCRTを施行した口腔癌175症例の有害事象

	Grade			
	0-2	3	4	3, 4（%）
粘膜炎	27	86	62	148（84.6）
皮膚炎	140	30	5	35（20.0）
好中球減少	142	31	2	33（18.9）
血小板減少	168	6	1	7（4.0）
貧血	146	26	3	29（16.6）
腎機能障害	175	0	0	0
発熱	162	13	0	13（7.4）
嘔吐	154	21	0	21（12.0）

表4　超選択的動注化学放射線療法後の生存率，局所制御率の報告

	部位（症例数）	生存率（%）		局所制御率（%）	
		3年	5年	3年	5年
Robbins et al.[14]	頭頸部（61）	56.2		57.2*	
Homma et al.[3]	頭頸部（43）	54.0		68.9*	
Kobayashi et al.[15]	口腔（22）	78.5	78.5		
本報告	口腔（175）	75.9	71.6	82.2	82.2

*局所・所属リンパ節制御率（%）

表5　超選択的動注化学放射線療法による有害事象の報告

Grade 3-5（%）	粘膜炎	皮膚炎	好中球減少	血小板減少	貧血	腎機能障害	発熱	嘔吐
Robbins et al.[14]	58	−	−	−	−	−	12	−
Homma et al.[3]	37.2	7.0	27.9	2.3	4.7	0	−	18.6
Kobayashi et al.[15]	68.2	−	86.4	4.5	1.8	−	−	0
本報告	84.6	20.0	18.9	4.0	16.6	0	7.4	12.0

化学放射線療法を行ったところ，grade 3，4の粘膜炎を68.2%認めた。Grade 3，4の好中球減少症，血小板減少症，貧血はぞれぞれ86.4%，4.5%，18.2%であった。これらはすべてSeldinger法でRobbinsら，Hommaらは毎週の抗癌剤の投与，Kobayashiらは4週毎の抗癌剤投与であった。われわれはgrade 3，4の粘膜炎を多く認めたが，これは連日の抗癌剤の動注を行っていることおよびDOCの動注を行っていることが影響していると思われた。粘膜炎に伴う嚥下障害も認めたが，治療終了後3か月以内にはすべての症例で経口摂取が可能となっている。

まとめ

今回われわれは進行口腔癌に対して根治的な逆行性超選択的動注化学放射線療法を施行し，治療効果，累積生存率，局所制御率について検討したところ，治療終了後の評価として91.4%にCRが得られ，5年累積生存率および局所制御率はそれぞれ71.6%と82.2%と良好な結果であった。今後さらに症例を増やし，根治的動注CCRT後の腫瘍残存，再発症例の検証を行い，治療成績の向上，予後の改善を目指していく予定である。

文献

1) Lee Y.Y., Dimery I.W., Tassel P.V., et al: Superselective intra-arterial chemotherapy of advanced paranasal sinus tumors. Arch Otolaryngol Head Neck Surg 115：503-511, 1989
2) Robbins K.T., Storniolo A.M., Kerber C, et al: Rapid superselective high-dose cisplatin infusion for advanced head and neck malignancies. Head & Neck 14：364-371, 1992
3) Homma A., Furuta Y., Suzuki F., et al: Rapid superselective high-dose cisplatin infusion with concomitant radiotherapy for advanced head and neck cancer. Head & Neck 27：65-71, 2005
4) 不破信和，伊藤善之，加藤恵理子他：頭頸部局所進行癌に対するCBDCA超選択的持続動注療法 頭頸部腫瘍 22：139-143, 1996
5) Tohnai I., Fuwa N., Hayashi Y., et al: New superselective intra-arterial infusion via superficial temporal artery for cancer of the tongue and tumour tissue platinum concentration after carboplatin (CBDCA) infusion. Oral Oncol 34：387-390, 1998
6) 岩井俊憲，光藤健司，福井敬文他：下顎歯肉癌に対する浅側頭動脈と後頭動脈よりの超選択的動注法—顎動脈と顔面動脈へのカテーテル同時留置術— 頭頸部癌 35：273-278, 2009
7) 藤内 祝，光藤健司，西口浩明他：浅側頭動脈よりの超選択的動注化学療法と放射線療法の連日同時併用療法—StageⅢ，Ⅳ口腔癌に対する術前治療— 頭頸部癌 31：413-418, 2005
8) Mitsudo K., Shigetomi T., Fujimoto Y., et al: Organ preservation with daily concurrent chemoradiotherapy using superselective intra-arterial infusion via a superficial temporal artery for T3 and T4 head and neck cancer infusion. Int J Radiat Oncol Biol Phys 79：1428-1435, 2011
9) Fuwa N., Ito Y., Matsumoto A., et al: A combination therapy of continuous superselective intraarterial carboplatin infusion and radiation therapy for locally advanced head and neck carcinoma. Phase I study Cancer 89：2099-2105, 2000
10) 藤内 祝，不破信和，光藤健司他：口腔癌に対する浅側頭動脈よりの新しい超選択的動注法—彎曲カテーテルとPUカテーテルを用いた方法— 頭頸部癌 31：39-44, 2005
11) Cmelak A.J., Li S., Goldwasser M.A., et al: Phase II trial of chemoradiation for organ preservation in resectable stage III or IV squamous cell carcinomas of the larynx or oropharynx: results of Eastern Cooperative Oncology Group Study E2399. J Clin Oncol 25：3971-3977, 2007
12) Taguchi T., Tsukuda M., Mikami Y., et al: Treatment results and prognostic factors for advanced squamous cell carcinoma of the head and neck treated with concurrent chemoradiotherapy. Auris Nasus Larynx 36：199-204, 2009
13) Boscolo-Rizzo P., Gava A., Marchiori C., et al: Functional organ preservation in patients with locoregionally advanced head and neck squamous cell carcinoma treated by platinum-based multidrug induction chemotherapy and concurrent chemoradiotherapy. Ann Oncol. 2011 in press
14) Robbins K.T., Kumar P., Harris J., et al: Supradose intra-arterial cisplatin and concurrent radiation therapy for the treatment of stage IV head and neck squamous cell carcinoma is feasible and efficacious in a multi-institutional setting: results of radiation therapy oncology group trial 9615. J Clin Oncol 23：1447-1454, 2005
15) Kobayashi W., Teh B.G., Sakaki H., et al: Superselective intra-arterial chemoradiotherapy with docetaxel-nedaplatin for advanced oral cancer. Oral Oncol 46：860-863, 2010